Neutrophil pyroptosis mediates pathology of *P.aeruginosa* lung Infection in the absence of the NADPH oxidase NOX2

Jae Chan Ryu

Department of Medical Science

The Graduate School, Yonsei University

Neutrophil pyroptosis mediates pathology of *P.aeruginosa* lung Infection in the absence of the NADPH oxidase NOX2

Directed by Professor Ji Hwan Ryu

The Doctoral Dissertation
submitted to the Department of Medical Science,
the Graduate School of Yonsei University
in partial fulfillment of the requirements for the degree of
Doctor of Philosophy

Jae Chan Ryu

December 2016

This certifies that the Doctoral Dissertation of Jae Chan Ryu is approved.

Thesis Supervisor: Ji Hwan Ryu

Thesis Committee Member : Sang Sun Yoon

Thesis Committee Member : Sung Jae Shin

Thesis Committee Member : Chae Gyu Park

Thesis Committee Member : Young Sam Kim

The Graduate School
Yonsei University

December 2016

ACKNOWLEDGEMENTS

It’s been over 5 years since I started a long journey to the degree of doctor of philosophy. Looking back on the past, I feel time flies so fast. I’d like to thank to my mentor, Professor Ji Hwan Ryu, who guided me from the beginning to complete my thesis. Professor Sang Sun Yoon, Professor Sung Jae Shin, Professor Chae Gyu Park and Professor Young Sam Kim helped me convincing myself to believe that my study has its own significance and advised in many ways.

My special thanks must go to Professor Joo-Heon Yoon, who provides such a wonderful environment for translational research and Professor Sang nam Lee, who supported and advised me whenever I was in trouble.

I’d like to share all great memories with my lab collegues whose big help and support made me cut through high seas.

Finally I’d like to appreciate to my parents who backed me up through whole time and I want to say thank to everyone around me.

TABLE OF CONTENTS

LIST OF FIGURES

ABSTRACT

Neutrophil pyroptosis mediates pathology of *P. aeruginosa* lung infection in the absence of the NADPH oxidase NOX2

Jae Chan Ryu

Department of Medical Science
The Graduate School, Yonsei University

(Directed by Professor Ji Hwan Ryu)

Nod-Like Receptor family, CARD domain-containing 4 (NLRC4)-inflammasome activation is required for efficient clearance of intracellular pathogens through caspsase-1-dependent pyroptosis in macrophages. Although neutrophils play a critical role in protection from *P. aeruginosa* infection, the mechanisms regulating NLRC4-inflammasome-mediated pyroptosis in neutrophils and its physiological role are largely unknown. I sought to determine the specific mechanisms regulating neutrophil pyroptosis in *P. aeruginosa* strain PAO1 (PAO1) lung infection and to identify the pathological role of this process. *Nox2*$^{-/-}$ models with reduced neutrophil antibacterial activity exhibited increased neutrophil pyroptosis, which was

mediated by flagellin, a pathogenic PAO1 component. I also demonstrated that PAO1-induced pyroptosis in neutrophils was dependent upon NLRC4 and Toll-like receptor 5 (TLR5), using animals deficient of *Nlrc4*$^{-/-}$, or *Tlr5*$^{-/-}$. This study reveals previously unknown mechanisms and physiological role of neutrophil pyroptosis during *P. aeruginosa* lung infection. Furthermore, those findings regarding neutrophil pyroptosis in the context of neutrophil dysfunction may explain the causes of acute infectious diseases in patients with incompetent neutrophils.

Key words: *pseudomonas aeruginosa*, neutrophil, pyroptosis, nlrc4, inflammasome, flagellin

Neutrophil pyroptosis mediates pathology of *P. aeruginosa* lung infection in the absence of the NADPH oxidase NOX2

Jae Chan Ryu

Department of Medical Science
The Graduate School, Yonsei University

(Directed by Professor Ji Hwan Ryu)

I. INTRODUCTION

P. aeruginosa is a major pathogen responsible for nosocomial pneumonia and is associated with high morbidity and mortality rates.[1-3] Since *P. aeruginosa* infections are most frequently seen in individuals with compromised immune systems, the host immune response is clearly essential in both preventing and controlling infection.[4,5] The bacterial protein flagellin is translocated to the cytosol, where it is efficiently recognized by NLRC4 (Nod-Like Receptor family, CARD domain-containing 4).[6-10] Several lines of evidence support an essential role for the NLRC4-coupled inflammasome in Caspase-1 (CASP1) activation in response to *Shigella flexneri*,[6] *Salmonella typhimurium*,[11] and *Legionella pneumophila*.[12] In these reports, mouse models

infected with these pathogens showed flagellin-induced activation of NLRC4 inflammasome/CASP1, leading to the secretion of proinflammatory cytokines such as IL-1β and IL-18 and induction of a rapid lytic form of inflammatory cell death known as pyroptosis. For host protection from pathogen invasion, interleukin-1β (IL-1β) and interleukin-18 (IL-18) induce phagocyte recruitment and activation.[13-15] In turn, pyroptosis releases the intracellular pathogens into the extracellular environment, exposing them to neutrophil-mediated destruction.[16-19] However, although these NLRC4/CASP1-dependent responses aid clearance of intracellular pathogens, NLRC4 activation by *P. aeruginosa* decreases the clearance of this pathogen and increases disease pathology in an acute lung infection.[20,21] In acute lung infection, neutrophils, rather than macrophages, are the first cell type recruited in large quantities to the site of infection and are thus involved in the initial clearance of infected cells. Genetic disorders leading to abnormal neutrophil function characterize up to 20% of all reported primary immune deficiencies.[22] Although neutrophils have been shown to play a critical role in the primary protection from pathogen infection, most studies of the NLRC4 inflammasome have focused on its regulatory role in the context of macrophages. However, NLRC4 was recently reported to be expressed in neutrophils and to be responsible for CASP1-dependent IL-1β secretion during *Salmonella* challenge.[11,23,24] Neutrophils are not likely to undergo pyroptosis because their

antibacterial activity is so strong that pathogens do not have enough time to proliferate and trigger pyroptosis. However, in conditions of neutrophil dysfunction in which antimicrobial activity is weakened, neutrophil pyroptosis might be induced by acute pathogen infection and play a critical role in the host immune response. Here we show that, when neutrophil antimicrobial activity is reduced, neutrophil pyroptosis is induced by *P. aeruginosa* infection, leading to higher inflammation and lung injury via an increased *P. aeruginosa* burden in the lung. We observed increased neutrophil pyroptosis in *Nox2*$^{-/-}$ mice, in which neutrophil antibacterial activity is low, both *in vitro* and *in vivo*.

II. MATERIALS AND METHODS

1. Animals

Male mice between 8 to 12 weeks of age were used in all experiments. *Nlrc4*$^{-/-}$ mice on the C57BL/6 background were kindly provided by professor Jong-Hwan Park (Chonnam National University, Gwangju, Korea). C57BL/6 mice were purchased from Orient Bio (Korea), whereas *Nox2*$^{-/-}$, *Nlrp3*$^{-/-}$, and *Tlr5*$^{-/-}$ mice on a C57BL/6 background were bred at the animal facility of Yonsei University. All mice were housed under SPF conditions until the start of each experiment. The animal ethics committee of the University of Yonsei approved all experimental protocols.

2. Preparation of *P.aeruginosa* strain PAO1 (PAO1)

PAO1 colonies were grown on a Luria-Bertani (LB) agar plate at 37°C overnight. The colonies were inoculated into 10 mL fresh LB medium and grown overnight at 37°C with shaking at 200 rpm. The overnight cultures were used to inoculate fresh LB medium and grown with aeration until reaching an OD 600 of 1. These cultures were then used as a source of bacteria for all experiments. GFP-tagged PAO1 strains were grown at 37°C in LB with carbenicillin (Gold biotechnology, St. Louis, MO, USA) (100 ug/ml), PAO1Δ*fliC* strains were grown at 37°C in LB with gentamicin (Gibco, Grand

Island, NY, USA) (20 ug/ml), and GFP-tagged PAO1Δ*fliC* strains were grown at 37°C in LB with carbenicillin (100 ug/ml) and gentamicin (20 ug/ml).

3. PAO1 infection model

Pulmonary infection of mice was performed by intranasal instillation with $4x10^5$ colony-forming units (cfu) of PAO1 or PAO1Δ*fliC*. Mock-infected mice were inoculated with phosphate-buffered saline (PBS). Mice were sacrificed at 12 or 24 hr after infection.

4. Flow cytometry

Cells obtained from BAL samples were counted and stained with Ly6G (eBiosciences, San Diego, CA, USA), FLICA-660 (Immunochemistry, Bloomington, MN, USA), Annexin V (Biovision, Milpitas, CA, USA), and PI (Biovision, Milpitas, CA, USA). Stained cells were analyzed with a FACSverse BD flow cytometer. Isolated murine neutrophils were identified using Ly6G (eBiosciences, San Diego, CA, USA) and isolated human neutrophils were identified using cd66b (BD Biosciences, San Jose, CA, USA). GFP-tagged PAO1 were used in conjunction with Ly6G to quantitate neutrophil uptake of bacteria. Pyroptotic neutrophils were detected using FLICA-660 and PI. Mitochondrial ROS were measured by staining cells with 5 uM MitoSOX (Invitrogen, Carlsbad, CA, USA) for 15 min at 37°C.

Mitochondrial membrane potential was measured by staining cells with 100 nM TMRE (Abcam, Cambridge, UK) for 20 min at 37°C.

5. Neutrophil and macrophage depletions

Neutrophils were depleted or mock-depleted by i.p. administration of 0.1 mg α-Ly6G antibody (endotoxin-free 1A8 clone, BioXcell, West Lebanon, NH, USA) or isotype control antibody (endotoxin-free 2A3 clone, BioXcell, West Lebanon, NH, USA). At 24 hr after antibody injection, mice were challenged intranasally with $4*10^5$ colony-forming units (cfu) of PAO1. Alveolar macrophages were depleted by intranasal instillation of clodronate liposomes or control liposomes (50 ul/mouse) (Formumax, Suite Palo Alto, CA, USA). Three days after the intranasal instillation of liposomes, $4*10^5$cfu of PAO1 were instilled.

6. Western blot analysis

Primary anti-caspase1 (Adipogen, San Diego, CA, USA) and anti-β-actin (Santa Cruz, Dallas, Texas, USA) (loading control) antibody were used. Murine bone marrow-derived neutrophils were lysed with lysis buffer (Invitrogen, Carlsbad, CA, USA) and the protein contents of the resultant extracts were quantified. Equal amounts were resolved by SDS-PAGE and transferred to nitrocellulose membranes (Millipore, Darmstadt, Germany).

The membranes were incubated with primary antibodies, followed by HRP-conjugated secondary antibodies. Immunoreactive bands were visualized using the ECL system (Animal Genetics, Tallahassee, FL, USA).

7. Preparation of mouse neutrophils

After cervical dislocation, both hind limbs were removed directly from each mouse and a single cell suspension w/o erythrocytes was generated. After centrifugation (1400 rpm/5 min/RT), neutrophils were isolated via negative selection by an autoMACS column (Miltenyi Biotec, Cologne, Germany). After negative selection of neutrophils, cells were stained with anti-Ly6G antibody and analyzed by flow cytometry to determine neutrophil purity (more than 95 % purity was obtained).

8. Isolation of human neutrophils from peripheral blood

Human neutrophils were isolated from the peripheral blood of healthy volunteers. Briefly, EDTA-treated blood was fractionated on a Ficoll-Paque Plus (GE Healthcare, Amersham, UK) gradient. Erythrocytes were lysed, and a >95% pure neutrophil population was obtained.

9. Cytokine production

Cytokine levels in BAL samples and cultured murine bone marrow-derived neutrophil supernatants were measured with a mouse IL-18 kit (MBL, Woburn, MA, USA) or a Duoset ELISA development kit for mouse TNF-α, IL-6, and IL-1β (R&D systems, Minneapolis, MN, USA). Cytokine levels in human neutrophil supernatants were measured with a human IL-18 kit (MBL, Woburn, MA, USA) or a Duoset ELISA development kit for human TNF-α and IL-1β.

10. Quantification of fibrin deposition

Formalin-fixed mouse left lung lobes were dehydrated gradually in ethanol, embedded in paraffin, and cut into 5 μm sections. Heat-induced epitope retrieval was then performed before staining. The tissue sections were permeabilized with 0.2% Triton X-100 for 10 min and blocked with phosphate-buffered saline (PBS) containing 1% BSA and 10% normal goat serum. Sections were then immunostained with anti-fibrin antibody (Dako, Glostrub, Denmark). After extensive washing with PBS, tissue sections were incubated with Alexa488-conjugated anti-rabbit IgG antibody. After washing with PBS, tissue sections were stained with DAPI and fibrin and DAPI colocalization was analyzed on a confocal microscope (Carl Zeiss; LSM 700).

11. Statistics

Comparisons of two samples were made by an unpaired Student's *t* test, whereas ANOVA followed by Tukey's post hoc test was performed to compare multiple samples.

The Kaplan-Meier log-rank test was used for the statistical analysis of survival experiments.

P values < 0.05 were considered statistically significant. In each figure legend, s.e.m. stands for the between-subjects standard error of the mean. All statistical analyses were performed using SPSS software (IBM).

III. RESULTS

1. *Nox2*$^{-/-}$ mice show increased bacterial burden, lung injury, and mortality after challenge with PAO1

To know the physiological role of NOX2 in acute lung infection, we first determined 4-day (d) survival rates in a lung infectious mouse model by pulmonary challenge with PAO1 ($4x10^5$ colony-forming units (cfu)) using NOX2-deficient mice (*Nox2*$^{-/-}$). Notably, *Nox2*$^{-/-}$ mice were more susceptible to PAO1 infection than their wild-type littermates (*Nox2*$^{+/+}$). At 3-4 d after PAO1 challenge, nearly all of the *Nox2*$^{-/-}$ mice had died, whereas all of the *Nox2*$^{+/+}$ mice survived beyond 3 d (Figure 1A). In accordance with their increased mortality, *Nox2*$^{-/-}$ mice had decreased pulmonary clearance of bacteria and significantly higher bacterial burdens in their bronchoalveolar lavage (BAL) fluid (Figure 1B). To determine whether the increased bacterial burden of *Nox2*$^{-/-}$ mice was accompanied by increased lung damage, we quantified the levels of protein and IgM in BAL fluid. *Nox2*$^{-/-}$ mice exhibited more lung injury than *Nox2*$^{+/+}$ mice at both 12 hr and 24 hr after PAO1 infection (Figures 1C and 1D). Fibrin deposition in the alveolar spaces of *Nox2*$^{-/-}$ mice was also much higher than in *Nox2*$^{-/-}$ mice (Figures 2A and B). Elevated levels of various inflammatory cytokines, including tumor necrosis factor-α (TNF-α) (Figure 3A), IL-1β (Figure 3B), and IL-6 (Figure 3C) were

also observed in *Nox2*$^{-/-}$ mice. These results indicate that NOX2 is critical for host protection against acute lung infection with PAO1 through clearance of bacteria.

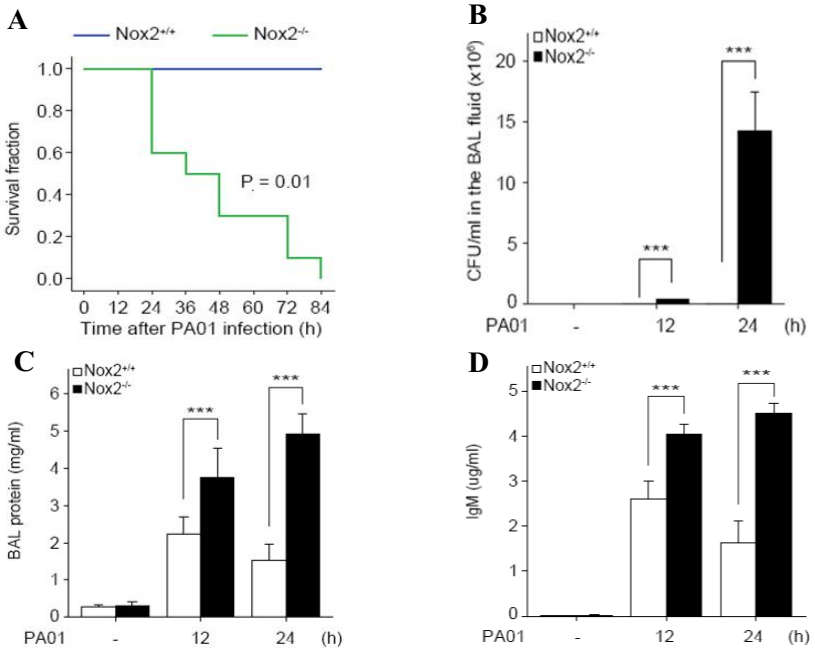

Figure 1. *Nox2*$^{-/-}$ mice show increased mortality, bacterial burden and lung injury upon PAO1 infection. (A-D) Mice were instilled intranasally with 4*10^5 cfu of PAO1. (A) The survival rates of *Nox2*$^{-/-}$ mice and *Nox2*$^{+/+}$ mice were monitored for 4 days (n=10). (B) *Nox2*$^{-/-}$ mice and *Nox2*$^{+/+}$ mice were sacrificed at 12 and 24 hr postinfection and the bacterial burdens in the BAL fluid were measured. (C) Protein and (D) IgM levels in the BAL fluid from *Nox2*$^{-/-}$ and *Nox2*$^{+/+}$ mice were determined at 12 and 24 hr after intranasal instillation of PAO1. ***P<0.001.

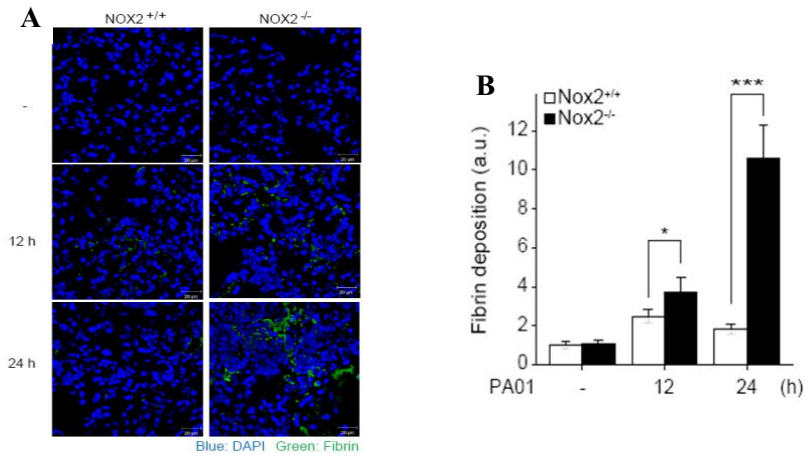

Figure 2. *Nox2*$^{-/-}$ mice show increased lung injury upon PAO1 infection.

(A and B) Fibrin deposits in lung tissue sections of *Nox2*$^{-/-}$ and *Nox2*$^{+/+}$ mice at 12 and 24 hr after intranasal instillation of PAO1. **P*<0.05; ****P*<0.001.

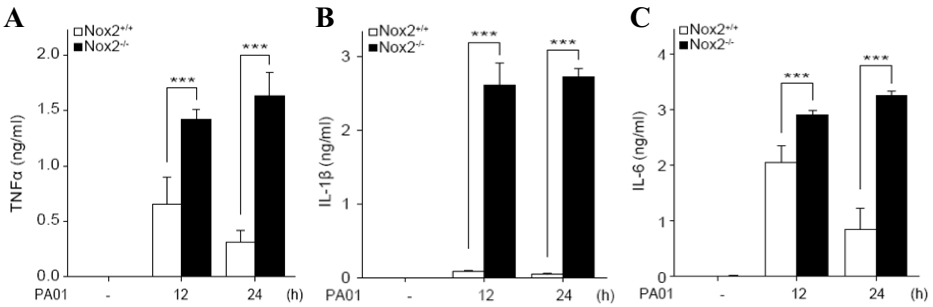

Figure 3. *Nox2*$^{-/-}$ mice show increased lung inflammation upon PAO1 infection. (A-C) Cytokine levels in BAL fluid after infection with PAO1. Levels of (A) TNF-α, (B) IL-1β, and (C) IL-6 in the BAL fluids from *Nox2*$^{-/-}$ and *Nox2*$^{+/+}$ mice were determined at 12 and 24 hr after intranasal instillation of PAO1. ***P<0.001.

2. Neutrophils, rather than macrophages, are essential for host protection during PAO1 lung infection

We next examined the numbers of intact neutrophils and macrophages in the bronchoalveolar spaces of *Nox2*$^{+/+}$ and *Nox2*$^{-/-}$ mice during PAO1 infection. In *Nox2*$^{+/+}$ mice, the number of neutrophils was significantly increased at 12 hr and decreased at 24 hr, while the number of macrophages was only slightly increased at 12 hr and 24 hr (Figure 4A). Interestingly, the number of neutrophils was dramatically decreased in *Nox2*$^{-/-}$ mice compared to that in *Nox2*$^{+/+}$ mice (Figure 4A). To determine whether neutrophils or macrophages are essential for bacteria clearance and host lung protection against PAO1 infection, we counted the CFUs and assessed the extent of lung injury in PAO1 infection after depleting neutrophils or macrophages, respectively. Administration of α-Ly6G antibody and clophosome efficiently depleted neutrophils (Figure 5A) and macrophages (Figure 5B), respectively, from the BAL fluid of wild-type (WT) mice. Much higher CFU counts (Figure 5C), levels of BAL protein (Figure 5D), and levels of immunoglobulin M (IgM) (Figure 5E) were detected in neutrophil-depleted mice compared with control mice, while none of these parameters were affected in macrophage-depleted mice (Figures 5C-E). Much higher levels of proinflammatory cytokines such as TNF-α, IL-1β, and IL-18 were observed in

neutrophil-depleted mice, while cytokine levels were not affected in macrophage-depleted mice (Figures 6A-C). These results indicate that neutrophil is critical for host protection against acute lung infection with PAO1 through clearance of bacteria.

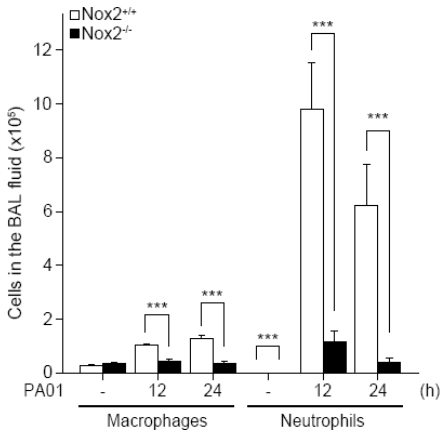

Figure 4. ***Nox2*$^{-/-}$ mice show fewer neutrophils in the bronchoalveolar space during PAO1 lung infection.** The numbers of macrophages and neutrophils in the BAL fluid were determined at 12 and 24 hr after intranasal instillation of $4*10^5$ cfu of PAO1. ***P<0.001.

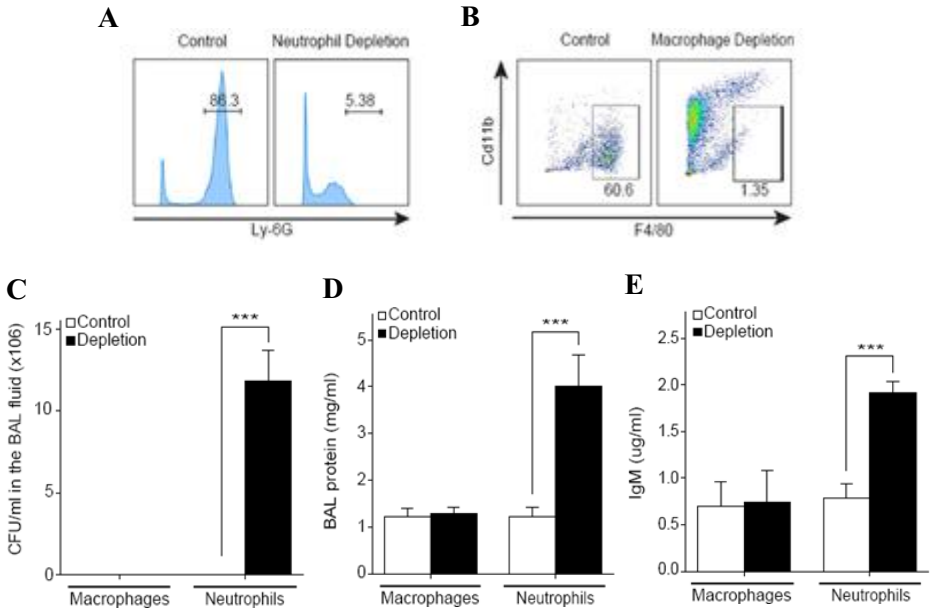

Figure 5. Neutrophils are major protector against acute lung infection with PAO1. (A) The extent of neutrophil depletion from BAL fluid was determined 8 hr after PAO1 infection by flow cytometry. (B) The extent of macrophage depletion from BAL fluid was determined without PAO1 infection by flow cytometry. (C-E) Bacterial burdens, lung injury, and cytokine levels in the BAL fluid from neutrophil-depleted mice after PAO1 infection. (C) Bacterial burdens, (D) BAL protein, (E) IgM levels in the BAL fluid from *Nox2*$^{-/-}$ and *Nox2*$^{+/+}$ mice were determined 24 hr after intranasal instillation of 4*10^5 cfu of PAO1. ***P<0.001.

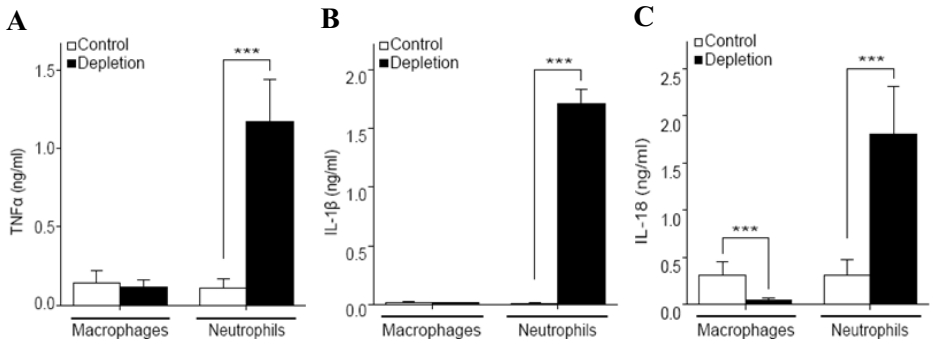

Figure 6. Neutrophil depleted mice show higher levels of proinflammatory cytokines during PAO1 lung infection. (A-C) Cytokine levels in the BAL fluid from neutrophil-depleted mice after PAO1 infection. (A) TNF-a, (B) IL-1β, and (C) IL-18 levels in the BAL fluid from *Nox2*$^{-/-}$ and *Nox2*$^{+/+}$ mice were determined 24 hr after intranasal instillation of 4*10^5 cfu of PAO1. ****P*<0.001.

3. Neutrophil pyroptosis is increased in *Nox2*$^{-/-}$ mice during acute lung infection

Since fewer intact neutrophils and higher PAO1 burdens were observed in the bronchoalveolar space of *Nox2*$^{-/-}$ mice compared to that of *Nox2*$^{+/+}$ mice during acute infection, we postulated that more neutrophils in *Nox2*$^{-/-}$ mice may undergo cell death than in *Nox2*$^{+/+}$. We first measured neutrophil cell death within the bronchoalveolar space through FACS analysis using propidium iodide (PI) or Annexin V staining of *Nox2*$^{+/+}$ or *Nox2*$^{-/-}$ mice upon PAO1 infection. The percentage of necrotic cells (PI^{+}/Annexin V^{+}) was dramatically increased in *Nox2*$^{-/-}$ neutrophils compared with *Nox2*$^{+/+}$ neutrophils upon infection, while the percentage of apoptotic cells (PI^{-} /Annexin V^{+}) was slightly increased in Nox2$^{-/-}$ neutrophils compared with *Nox2*$^{+/+}$ neutrophils (Figures 7A and B). We next hypothesized that pyroptosis, a lytic form of programmed cell death, is induced in neutrophils in PAO1-infected *Nox2*$^{-/-}$ mice. We compared the levels of neutrophil pyroptosis in *Nox2*$^{+/+}$ versus *Nox2*$^{-/-}$ mice upon PAO1 infection using a FACS strategy to detect active CASPASE1 (CASP1)-positive and PI-positive cells. In *Nox2*$^{+/+}$ mice, the percentage of pyroptotic neutrophils was extremely low at 24 hr after PAO1 infection (about 0.7%), while neutrophils from *Nox2*$^{-/-}$ mice showed marked pyroptotic cell death, with more than a 15-fold increase (approximately 11%) in same condition (Figures 8A and B). A higher number

of neutrophils showing the necrotic phenotype, including loss of cell membrane integrity and release of cellular contents, and an increased load of extracellular bacteria were observed in the bronchoalveolar space of infected *Nox2*$^{-/-}$ mice compared with *Nox2*$^{+/+}$ mice (Figures 9A and B). These results indicate that NOX2 suppresses neutrophil pyroptosis during PAO1 lung infection.

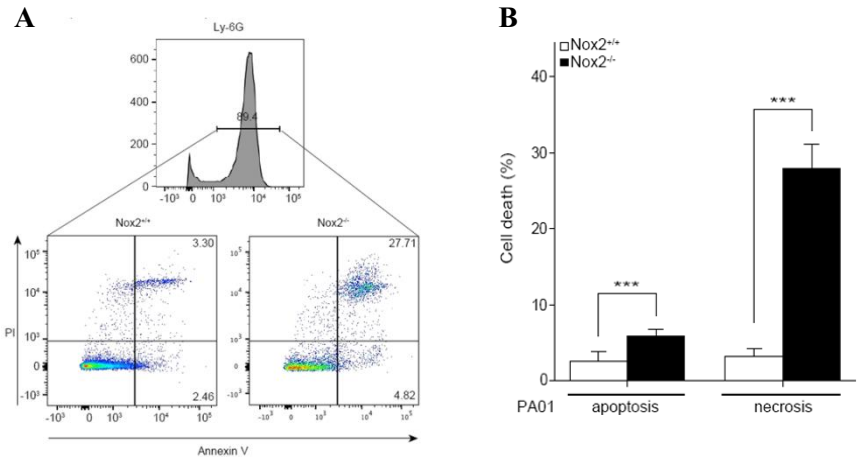

Figure 7. Cell death of neutrophils is increased in the lungs of *Nox2*$^{-/-}$ mice during PAO1 infection. (A and B) Neutrophil cell death in the BAL fluid from PAO1-infected mice. (A) Representative flow cytometry plots and (B) percentages of neutrophil cell death in the BAL fluids from *Nox2*$^{-/-}$ and *Nox2*$^{+/+}$ mice were determined 24 hr after intranasal instillation of $4*10^5$ cfu of PAO1. ***P<0.001.

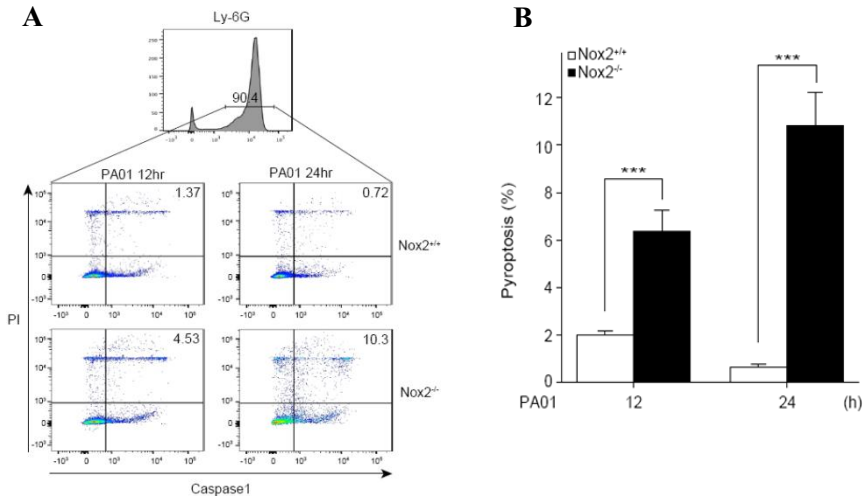

Figure 8. Neutrophil pyroptosis is increased in the lungs of *Nox2*$^{-/-}$ mice during PAO1 infection. (A and B) Neutrophil pyroptosis in the BAL fluid from PAO1-infected mice. (A) Representative flow cytometry plots and (B) percentages of neutrophil pyroptosis in the BAL fluids from *Nox2*$^{-/-}$ and *Nox2*$^{+/+}$ mice were determined at 12 and 24 hr after intranasal instillation of $4*10^5$ cfu of PAO1. ***P<0.001.

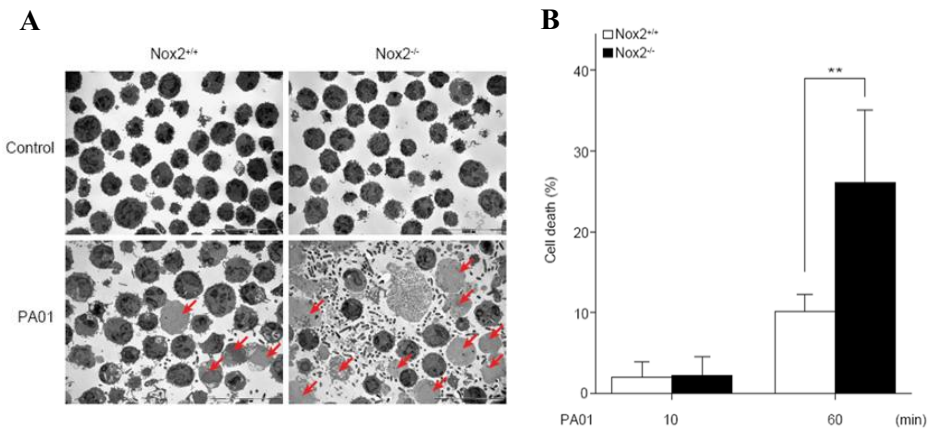

Figure 9. Neutrophils derived from *Nox2*$^{-/-}$ mice show increased necrotic cell death during PAO1 infection. (A) Transmission electron microscopy image of the morphological changes in bone marrow-derived neutrophils (BMDNs) and (B) percentages of dead BMDNs from *Nox2*$^{-/-}$ and *Nox2*$^{+/+}$ mice were determined 1 hr after infection with PAO1 (MOI 20). Scale bar = 20 um. ***P*<0.01.

4. Neutrophils derived from *Nox2*$^{-/-}$ mice show higher bacterial burdens and more pyroptosis upon PAO1 infection

We next investigated whether the increase in neutrophil pyroptosis in *Nox2*$^{-/-}$ mice depends on the amount of neutrophil-internalized bacteria. We first infected BMDNs extracted from *Nox2*$^{+/+}$ or *Nox2*$^{-/-}$ mice with green fluorescent protein (GFP)-tagged PAO1 (PAO1-GFP) to determine the efficiency of PAO1-GFP infection. The number of *Nox2*$^{-/-}$ BMDNs containing PAO1-GFP was not significantly different than that of *Nox2*$^{+/+}$ BMDNs with PAO1-GFP at 10 m postinfection (Figures 10A and B). However, The number of *Nox2*$^{-/-}$ BMDNs containing PAO1-GFP were more increased than that of *Nox2*$^{+/+}$ BMDNs containing PAO1-GFP at 60 m postinfection (Figures 10A and B), indicating that NOX2 is responsible for clearance of neutrophil-ingested PAO1, but not for initial PAO1 uptake. In accordance with the rates of PAO1 uptake, pyroptosis was significantly increased in *Nox2*$^{-/-}$ BMDNs with PAO1-GFP at 60 m, but not 10 m, postinfection (Figures 11A and B). Western blot analysis confirmed that CASP1 is more efficiently processed in *Nox2*$^{-/-}$ BMDNs than in *Nox2*$^{+/+}$ BMDNs, as evidence by the increased levels of its mature form (CASP1 p20) at 30 m and 60 m postPAO1 infection (Figure 12A). Furthermore, *Nox2*$^{-/-}$ BMDNs had secreted more IL-1β than *Nox2*$^{+/+}$ BMDNs at 60 m after PAO1 infection (Figure 12B). However, secretion of IL-18, another CASP1-dependent cytokine, was barely detected

in *Nox2*$^{-/-}$ and *Nox2*$^{+/+}$ BMDNs at 60 m after PAO1 infection (data not shown). These results indicate that the increased bacterial burden in *Nox2*$^{-/-}$ BMDNs contributes to the increased pyroptosis.

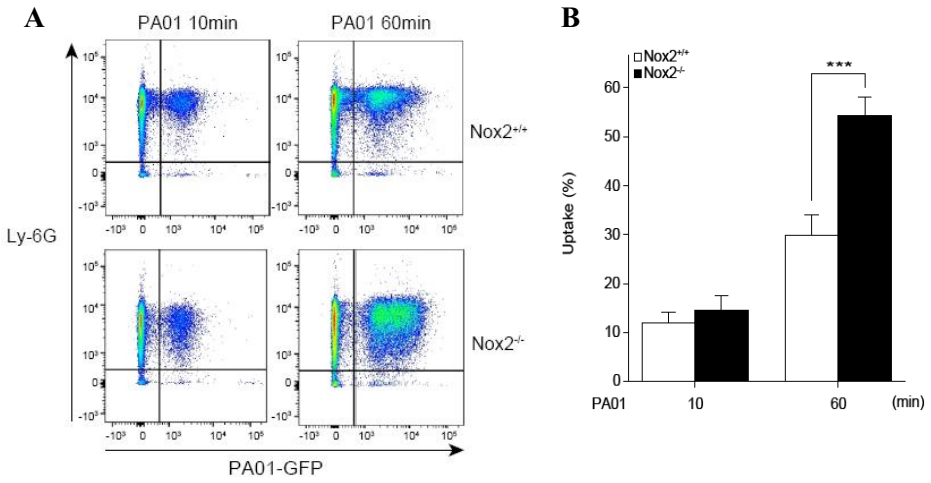

Figure 10. Neutrophils derived from *Nox2*$^{-/-}$ mice show higher bacterial burdens upon PAO1 infection. (A-B) Bone marrow-derived neutrophils (BMDNs) extracted from *Nox2*$^{-/-}$ mice and *Nox2*$^{+/+}$ mice were infected with GFP-tagged PAO1 (PAO1-GFP). (A) Representative flow cytometry plots and (B) percentages of BMDN uptake in *Nox2*$^{-/-}$ and *Nox2*$^{+/+}$ mice were determined at 10 and 60 m after infection with PAO1-GFP (MOI 20). ***P<0.001.

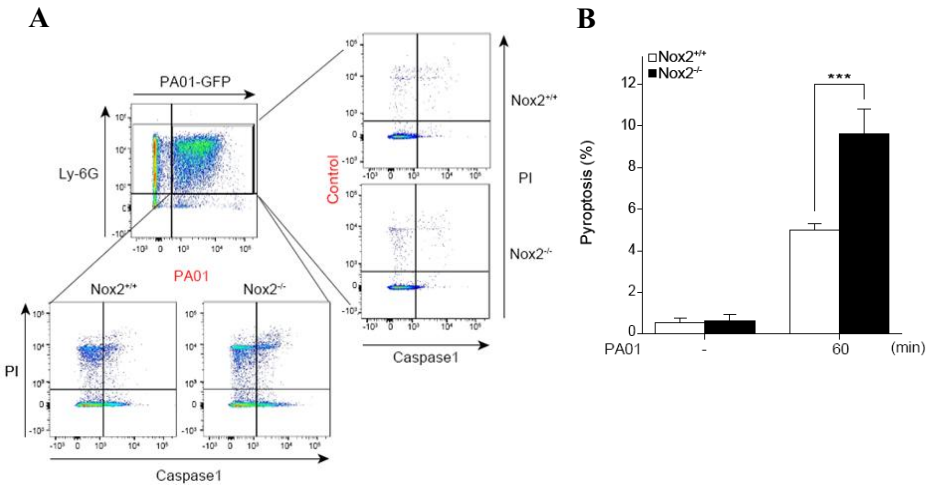

Figure 11. Neutrophils derived from *Nox2*$^{-/-}$ mice show increased pyroptosis upon PAO1 infection. (A-B) Bone marrow-derived neutrophils (BMDNs) extracted from *Nox2*$^{-/-}$ mice and *Nox2*$^{+/+}$ mice were infected with GFP-tagged PAO1 (PAO1-GFP). (A) Representative flow cytometry plots and (B) percentages of pyroptotic BMDNs, including PAO1-GFP, in *Nox2*$^{-/-}$ and *Nox2*$^{+/+}$ mice were determined 1 hr after infection with PAO1-GFP (MOI 20). ***P<0.001.

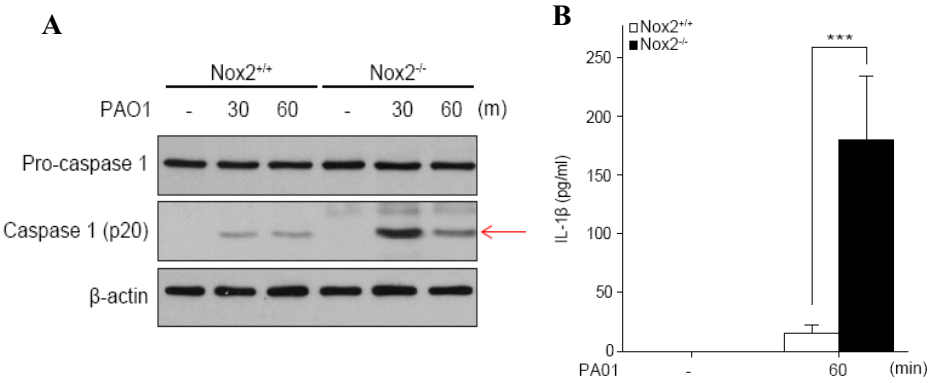

Figure 12. Neutrophils derived from *Nox2*$^{-/-}$ mice show higher CASP1 activation and IL-1β secretion upon PAO1 infection. (A and B) BMDNs were infected with PAO1 (MOI 20). Cell extracts and their supernatants were harvested at 30 and 60 m postinfection. (A) Expression of cleaved CASP1 in cell extracts was detected by western blotting. (B) The levels of IL-1β in cell supernatants were detected by ELISA. ***P<0.001.

5. PAO1 infection-induced mitochondrial ROS is responsible for neutrophil pyroptosis

To examine the effect of PAO1 infection on mitochondrial integrity in neutrophils, we evaluated the functional mitochondrial pool in PAO1-infected BMDNs. To this end, we used tetramethylrhodamine ethyl ester (TMRE), a fluorescent probe sensitive to mitochondrial membrane potential, to assess mitochondrial depolarization. More mitochondrial depolarization occurred in *Nox2*$^{-/-}$ BMDNs compared with *Nox2*$^{+/+}$ BMDNs upon PAO1 infection, while it was not affected in the absence of PAO1 infection (Figures 13A and B). In accordance with these TMRE results, the level of mitochondrial ROS in *Nox2*$^{-/-}$ BMDNs was much higher than that in *Nox2*$^{+/+}$ BMDNs upon PAO1 infection (Figures 13C and D). We quantified pyroptosis in *Nox2*$^{+/+}$ and *Nox2*$^{-/-}$ BMDNs upon PAO1 infection after treating cells with Mito-Tempo, a mitochondrial ROS scavenging reagent. The PAO1-mediated increase in pyroptosis in *Nox2*$^{-/-}$ BMDNs was significantly decreased in the presence of Mito-Tempo (Figure 14A). The increased levels of CASP1 activation and IL-1β in *Nox2*$^{-/-}$ BMDNs were also blunted in the presence of Mito-Tempo (Figure 14B and C).

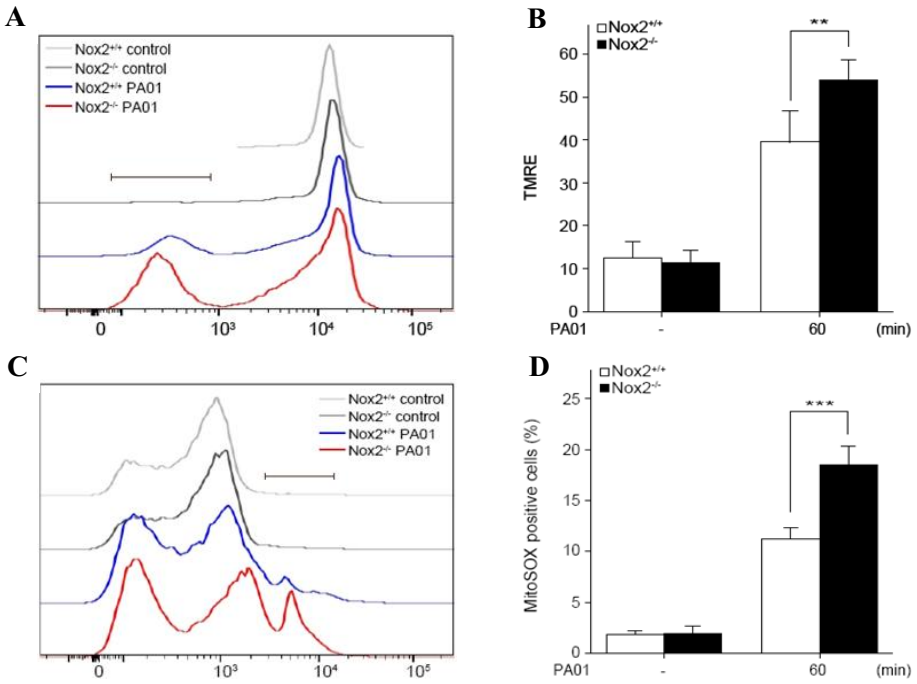

Figure 13. PAO1 infection damages mitochondria and generates mitochondrial ROS. (A and B) The levels of TMRE and (C and D) mitochondrial ROS in BMDNs from *Nox2*$^{-/-}$ and *Nox2*$^{+/+}$ mice were determined 1 hr after infection with PAO1 (MOI 20). ***P*<0.01;****P*<0.001.

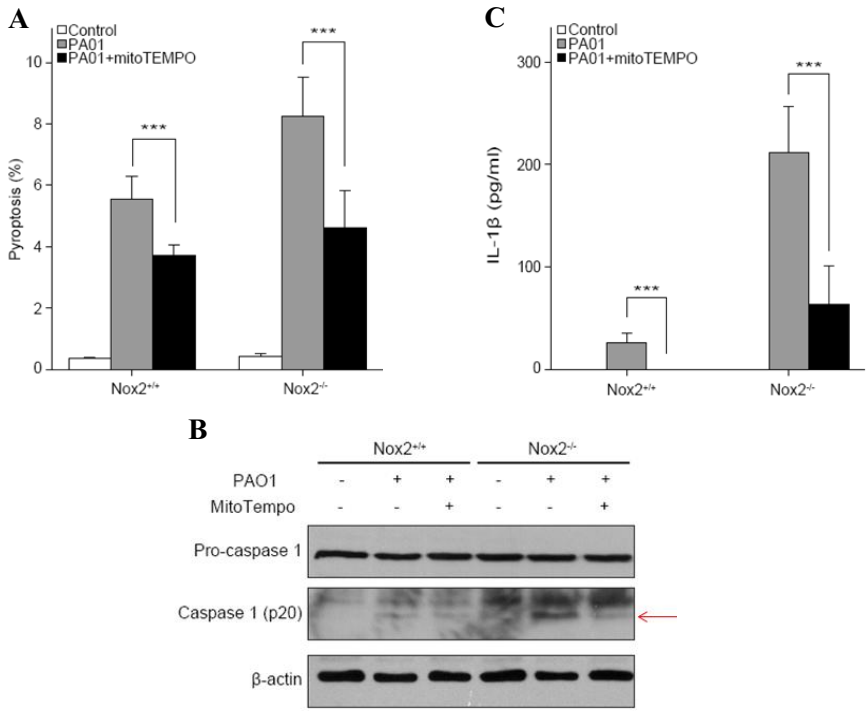

Figure 14. PAO1 infection generates mitochondrial ROS and induces neutrophil pyroptosis. (A) The levels of pyroptosis in BMDNs from *Nox2*$^{-/-}$ and *Nox2*$^{+/+}$ mice were determined 1 hr after infection with PAO1 (MOI 20) alone or with PAO1 in the presence of Mito-TEMPO. (B and C) BMDNs were infected with PAO1 (MOI 20) alone or PAO1 in the presence of Mito-TEMPO; cell extracts and supernatants were harvested at 1 hr postinfection. (B) Expression of cleaved CASP1 in cell extracts was detected by western blotting. (C) The levels of IL-1β in the cell supernatants were detected by ELISA. ***P<0.001.

6. PAO1-stimulated neutrophil pyroptosis depends on the NLRC4 inflammasome

To know the role of NLRC4 in neutrophil pyroptosis in our system, we infected *Nlrc4*$^{+/+}$ and *Nlrc4*$^{-/-}$ BMDNs with two different doses of PAO1-GFP, and evaluated each BNDNs containing PAO1-GFP. The increase in pyroptosis of *Nlrc4*$^{+/+}$ BMDNs containing PAO1-GFP was significantly decreased in *Nlrc4*$^{-/-}$ BMDNs (Figure 15A). However, the numbers of *Nlrc4*$^{-/-}$ BMDNs containing PAO1-GFP were not different than those of *Nlrc4*$^{+/+}$ BMDNs at both 10 m and 60 m after infection (Figure 15B). The increased secretion of IL-1β in *Nlrc4*$^{+/+}$ BMDNs was also significantly blunted in *Nlrc4*$^{-/-}$ BMDNs (Figure 15C). In contrast, the increase in pyroptosis and the number of BMDNs with PAO1-GFP in *Nlrp3*$^{+/+}$ BMDNs were not changed in *Nlrp3*$^{-/-}$ BMDNs (Figures 16A and B). However, increased secretion of IL-1β in *Nlrp3*$^{+/+}$ BMDNs was significantly decreased in *Nlrp3*$^{-/-}$ BMDNs (Figure 16C). These findings suggest the existence of a signaling pathway upstream of NLR family, Pyrin Domain Containing 3 (NLRP3) responsible for IL-1β secretion, but not pyroptosis, in PAO1-infected BMDNs.

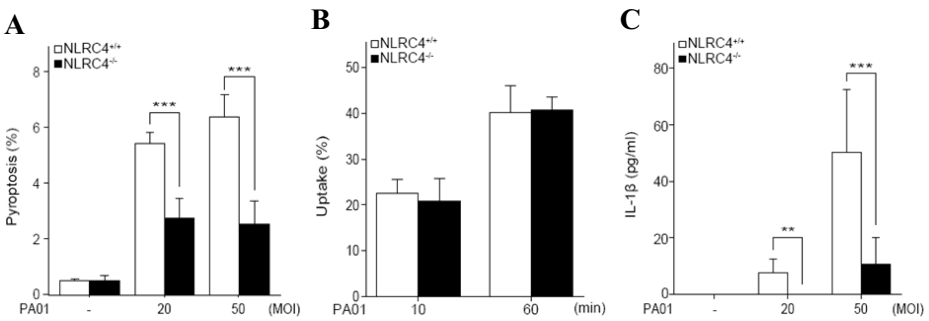

Figure 15. Neutrophil pyroptosis induced by PAO1 infection is mediated by the NLRC4 inflammasome. (A-C) BMDNs from *Nlrc4*$^{-/-}$ and *Nlrc4*$^{+/+}$ mice infected with PAO1-GFP. (A) The percentages of pyroptotic BMDNs, including PAO1-GFP, from *Nlrc4*$^{-/-}$ and *Nlrc4*$^{+/+}$ mice were determined 1 hr after infection with PAO1-GFP (MOI 20, 50). (B) The percentages of BMDNs uptake from *Nlrc4*$^{-/-}$ and *Nlrc4*$^{+/+}$ mice were determined at 10 and 60 m after infection with PAO1-GFP (MOI 20). (C) IL-1β levels were detected in the supernatants of BMDNs from *Nlrc4*$^{-/-}$ and *Nlrc4*$^{+/+}$ mice after infection with PAO1 (MOI 20, 50). $^{**}P<0.01$;$^{***}P<0.001$.

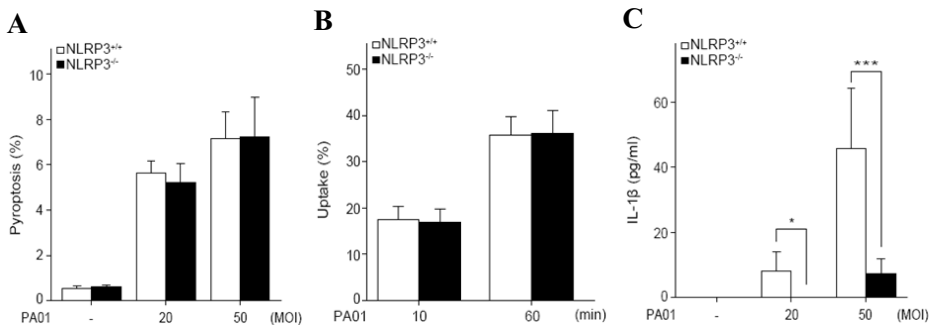

Figure 16. Neutrophil pyroptosis induced by PAO1 infection is not mediated by the NLRP3 inflammasome. (A-C) BMDNs from *Nlrp3*$^{-/-}$ and *Nlrp3*$^{+/+}$ mice infected with PAO1-GFP. (A) The percentages of pyroptotic BMDNs, including PAO1-GFP, from *Nlrp3*$^{-/-}$ and *Nlrp3*$^{+/+}$ mice were determined 1 hr after infection with PAO1-GFP (MOI 20, 50). (B) The percentages of BMDNs uptake from *Nlrp3*$^{-/-}$ and *Nlrp3*$^{+/+}$ mice were determined at 10 and 60 m postinfection with PAO1-GFP (MOI 20). (C) IL-1β levels were detected in the supernatants of BMDNs from *Nlrp3*$^{-/-}$ and *Nlrp3*$^{+/+}$ mice 1 hr after infection with PAO1 (MOI 20, 50). **P*<0.05; ****P*<0.001.

7. TLR5 contributes to neutrophil pyroptosis by regulating PAO1 uptake

Given that, in addition to NLRC4, TLR5 is a known receptor for PAO1 flagellin,[25,26] we wondered whether TLR5 is involved in PAO1-stimulated pyroptosis. The increase in pyroptosis in *Tlr5*$^{+/+}$ BMDNs was slightly blunted in *Tlr5*$^{-/-}$ BMDNs (Figure 17A). In contrast to the results obtained with *Nlrc4*$^{-/-}$ BMDNs, fewer numbers of *Tlr5*$^{-/-}$ BMDNs with PAO1-GFP were observed compared with *Tlr5*$^{+/+}$ BMDNs with PAO1-GFP at both 10 and 60 min after infection (Figure 17B). These data suggest that the decreased pyroptosis in *Tlr5*$^{-/-}$ BMDNs might be due to the decrease in initial uptake of PAO1-GFP in *Tlr5*$^{-/-}$ BMDNs. Moreover, the increase in IL-1β secretion in *Tlr5*$^{+/+}$ BMDNs was dramatically decreased in *Tlr5*$^{-/-}$ BMDNs (Figure 17C).

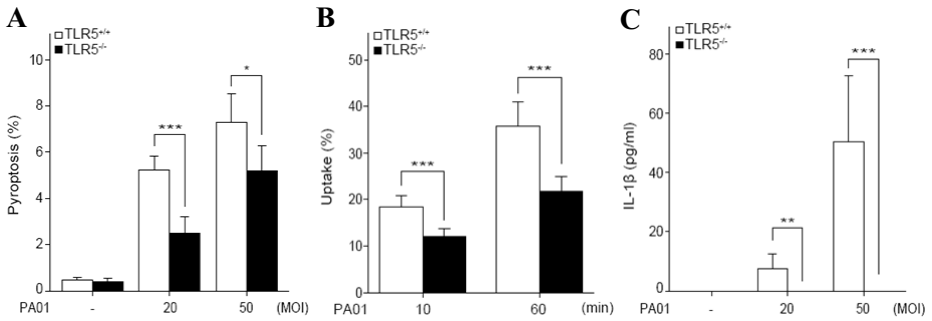

Figure 17. TLR5 contributes to PAO1-mediated induction of neutrophil pyroptosis. (A-C) BMDNs from *Tlr5*$^{-/-}$ and *Tlr5*$^{+/+}$ mice were infected with PAO1-GFP. (A) The percentages of pyroptotic BMDNs, including PAO1-GFP, from *Tlr5*$^{-/-}$ and *Tlr5*$^{+/+}$ mice were determined 1 hr after infection with PAO1-GFP (MOI 20, 50). (B) The percentages of BMDNs uptake from *Tlr5*$^{-/-}$ and *Tlr5*$^{+/+}$ mice were determined at 10 and 60 m after infection with PAO1-GFP (MOI 20). (C) IL-1β levels were detected in the supernatants of BMDNs from *Tlr5*$^{-/-}$ and *Tlr5*$^{+/+}$ mice 1 hr after infection with PAO1 (MOI 20, 50). **P*<0.05; ***P*<0.01;****P*<0.001.

8. PAO1 flagellin is required for neutrophil pyroptosis upon infection

Since we found that both NLRC4 and TLR5 are involved in PAO1-stimulated neutrophil pyroptosis, we hypothesized that PAO1 flagellin is responsible for the induction of neutrophil pyroptosis upon infection. We observed that neutrophils infected with a PAO1 mutant devoid of flagellin production (PAO1Δ*fliC*) exhibited significantly decreased pyroptosis compared with neutrophils infected with WT PAO1 (Figure 18A). The number of BMDNs with PAO1Δ*fliC*-GFP was also lower than the number of BMDNs infected with PAO1-GFP (Figure 18B). Moreover, the level of IL-1β secretion induced by PAO1Δ*fliC* infection was much lower than that induced by PAO1 infection (Figure 18C). Since the *P. aeruginosa* type 3 secretion system (T3SS) is responsible for NLRC4-inflammasome activation in macrophages,[20] we determined the extent of neutrophil pyroptosis and pathogen uptake upon infection with PAO1ΔT3SS-GFP. The levels of pyroptosis and neutrophil uptake in the context of PAO1ΔT3SS-GFP infection were not significantly different than those in the context of PAO1-GFP infection (Figures 19A and B), while the level of IL-1β secretion stimulated by PAO1ΔT3SS infection was much lower than that stimulated by PAO1 infection (Figure 19C).

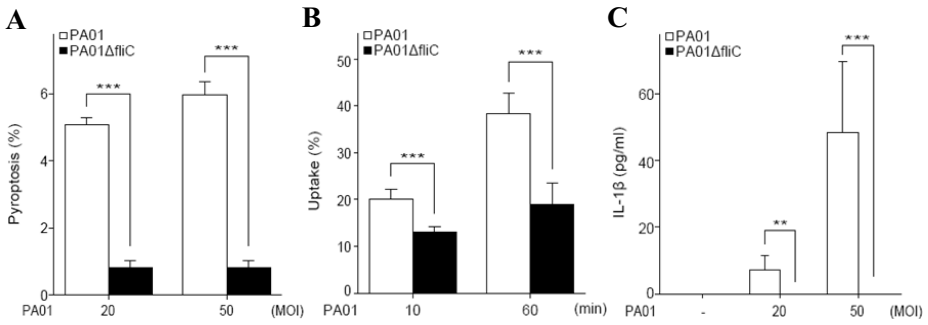

Figure 18. PAO1 flagellin is required for neutrophil pyroptosis upon PAO1 infection. (A-C) BMDNs from WT mice were infected with PAO1-GFP and PAO1Δ*fliC*-GFP. (A) The percentages of pyroptotic BMDNs, including PAO1-GFP, from WT mice were determined 1 hr after infection with PAO1-GFP and PAO1Δ*fliC*-GFP (MOI 20, 50). (B) The percentages of BMDNs uptake from WT mice were determined at 10 and 60 m after infection with PAO1-GFP and PAO1Δ*fliC*-GFP (MOI 20). (C) IL-1β levels were detected in the supernatants of BMDNs from WT mice 1 hr after infection with PAO1-GFP and PAO1Δ*fliC*-GFP (MOI 20, 50). $^{**}P<0.01$;$^{***}P<0.001$.

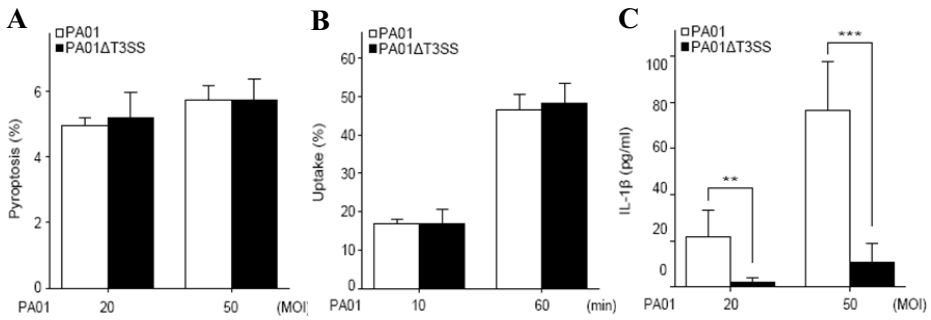

Figure 19. PAO1 T3SS is not required for neutrophil pyroptosis upon PAO1 infection. (A-C) BMDNs from WT mice were infected with PAO1-GFP and PAO1ΔT3SS-GFP. (A) The percentages of pyroptotic BMDNs, including PAO1-GFP, from WT mice were determined 1 hr after infection with PAO1-GFP and PAO1ΔT3SS-GFP (MOI 20, 50). (B) The percentages of BMDNs with uptake of PAO1-GFP and PAO1ΔT3SS-GFP from WT mice were determined at 10 and 60 m after infection (MOI 20). (C) IL-1β levels were detected in the supernatants of BMDNs from WT mice 1 hr after infection with PAO1-GFP and PAO1ΔT3SS-GFP (MOI 20, 50). $^{**}P<0.01$;$^{***}P<0.001$.

9. PAO1 flagellin is responsible for neutrophil pyroptosis and lung injury during acute lung infection

To investigate the physiological role of PAO1 flagellin in our acute lung infection mouse model, we challenged *Nox2*$^{+/+}$ or *Nox2*$^{-/-}$ mice with PAO1 or PAO1Δ*fliC*. In *Nox2*$^{+/+}$ mice, the percentage of pyroptotic neutrophils was extremely low (about 1%) upon infection with either PAO1 or PAO1Δ*fliC*, while the PAO1-stimulated increase in pyroptosis in *Nox2*$^{-/-}$ mice (about 10%) was significantly decreased upon PAO1Δ*fliC* infection (about 6%) (Figure 20A). The increased PAO1 CFUs in the BAL fluid of *Nox2*$^{-/-}$ mice was also decreased by using PAO1Δ*fliC* (Figure 20B). In accordance with the lower bacterial burden of PAO1Δ*fliC*, the increased levels of lung injury markers such as BAL protein (Figure 20C) and IgM (Figure 20D) in *Nox2*$^{-/-}$ mice induced by PAO1 infection were blunted in the context of PAO1Δ*fliC* infection. Lower levels of inflammatory cytokines such as TNFα (Figure 21A), IL-1β (Figure 21B), and IL-18 (Figure 21C) were observed in *Nox2*$^{-/-}$ mice infected with PAO1Δ*fliC* than in mice infected with PAO1.

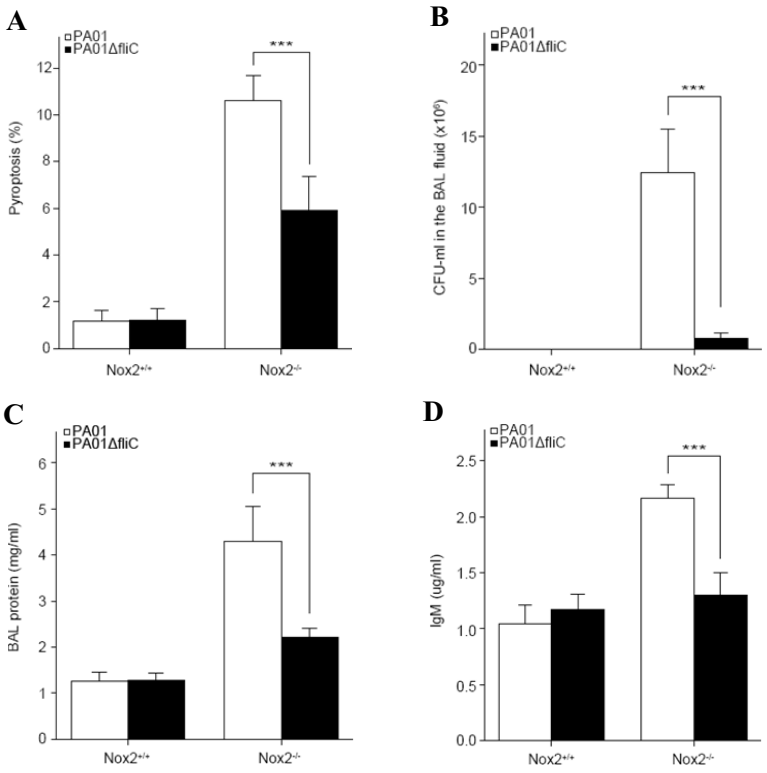

Figure 20. PAO1 flagellin is responsible for lung injury during PAO1 infection. (A-D) Mice were instilled intranasally with $4*10^5$ cfu of PAO1 or PAO1Δ*fliC*. (A) The percentages of pyroptotic neutrophils in the BAL fluids from *Nox2*$^{-/-}$ and *Nox2*$^{+/+}$ mice were determined 24 hr after intranasal instillation of PAO1 or PAO1Δ*fliC*. (B) *Nox2*$^{-/-}$ and *Nox2*$^{+/+}$ mice were sacrificed at 24 hr postinfection with PAO1 or PAO1Δ*fliC* and the bacterial burdens, (C) protein and (D) IgM levels in the BAL fluid were measured. ***P<0.001.

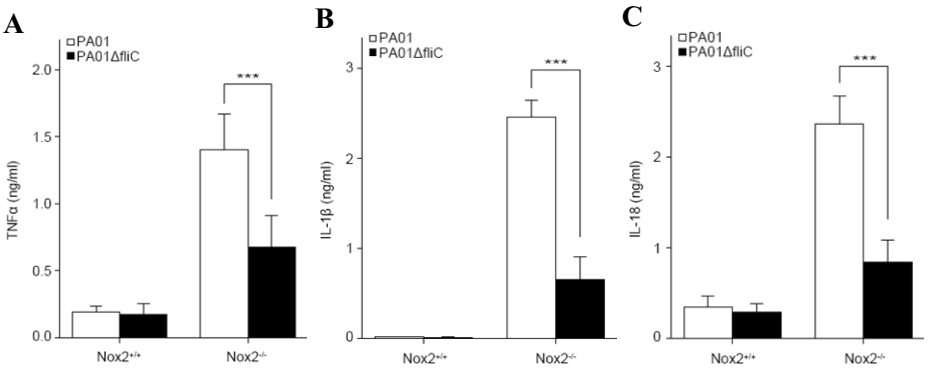

Figure 21. PAO1 flagellin induces lung inflammation during PAO1 infection. (A-C) Mice were instilled intranasally with $4*10^5$ cfu of PAO1 or PAO1Δ*fliC*. The levels of (A) TNF-α, (B) IL-1β, and (C) IL-18 in the BAL fluids from *Nox2*$^{-/-}$ and *Nox2*$^{+/+}$ mice were determined 24 hr after intranasal instillation of PAO1 or PAO1Δ*fliC*. ***P<0.001.

10. PAO1 flagellin mediates pyroptosis in infected human neutrophils

To investigate whether our *in vivo* and *in vivo* results were mirrored in human neutrophils, we investigated whether PAO1 flagellin mediated pyroptosis in human neutrophils. To this end, we infected human neutrophils with PAO1 or PAO1Δ*fliC* and quantified pyroptosis at 60 m postinfection. Neutrophils infected with PAO1Δ*fliC* exhibited significantly decreased pyroptosis compared with neutrophils infected with PAO1 (Figure 22A). In contrast, the number of human neutrophils with PAO1-GFP was not significantly different than that with PAO1Δ*fliC*-GFP (Figure 22B). Furthermore, PAO1Δ*fliC* infection resulted in reduced IL-18 secretion compared with PAO1 infection (Figure 22C). However, IL-1β secretion was hardly detected in human neutrophils at 60 m after PAO1 infection (data not shown). We also used time-lapse video microscopy to track pyroptosis in live human neutrophils infected with either PAO1-GFP or PAO1Δ*fliC*-GFP. Cleaved CASP1 (red) started to appear in human neutrophils throughout the cytoplasm at 20 m after PAO1 infection. The infected neutrophils had a swollen appearance at 40 min and underwent cell death by 60 min after PAO1 infection. In contrast, cleaved CASP1 and cell death were barely observed in neutrophils infected with PAO1Δ*fliC*-GFP (Figure 22D). These results

indicate that flagellin is responsible for pyroptosis in human neutrophils upon PAO1 infection.

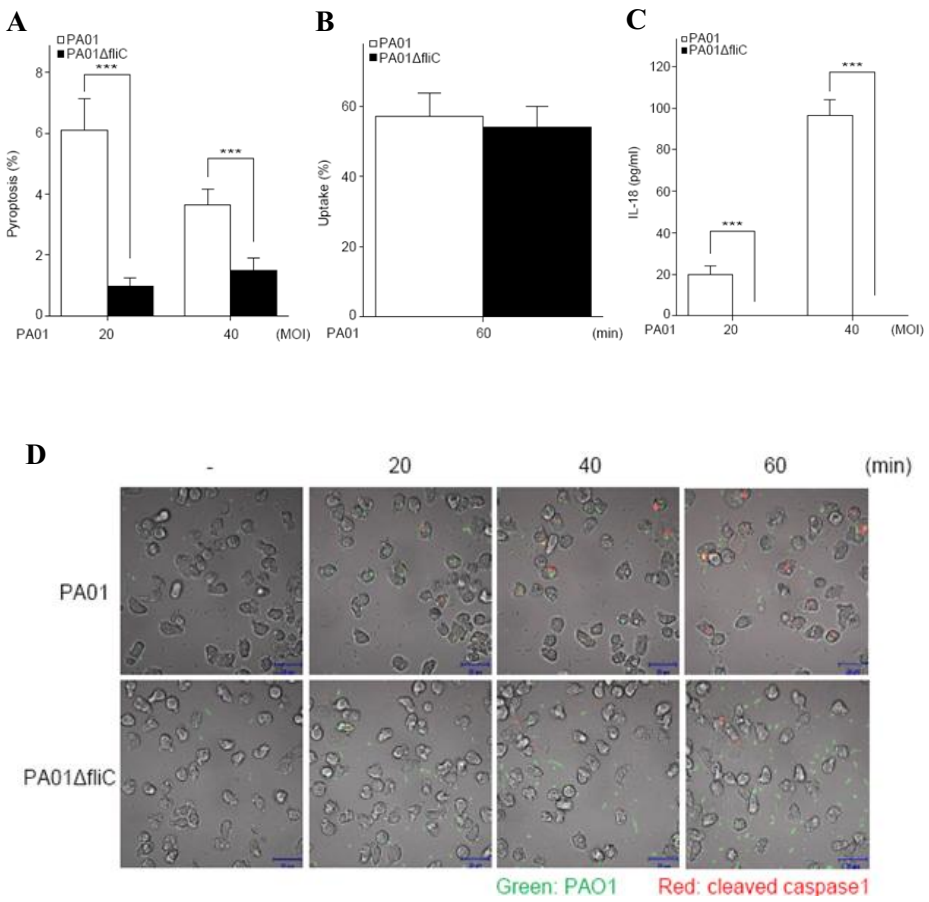

Figure 22. PAO1 flagellin induces pyroptosis in infected human neutrophils. (A-D) Human neutrophils were infected with PAO1-GFP or PAO1Δ*fliC*-GFP. (A) The percentages of pyroptotic human neutrophils, including PAO1-GFP, were determined 1 hr after infection with PAO1-GFP or PAO1Δ*fliC*-GFP (MOI 20, 40). (B) The percentages of human neutrophils with PAO1-GFP or PAO1Δ*fliC*-GFP uptake were determined 1 hr after infection (MOI 20). (C) IL-18 levels were detected in the supernatants of human neutrophils 1 hr after infection with PAO1-GFP or PAO1Δ*fliC*-GFP (MOI 20, 40). (D) A series of images from a representative live-cell video microscopy experiment showing human neutrophils, PAO1, and CASP1 activity during uptake and after uptake. PAO1 continued to grow within human neutrophils, which can result in cell lysis. Active CASP1 was detected with the far-red FLICA 660 probe and cells were infected with GFP-tagged PAO1 or GFP-tagged PAO1Δ*fliC*. ***$P<0.001$.

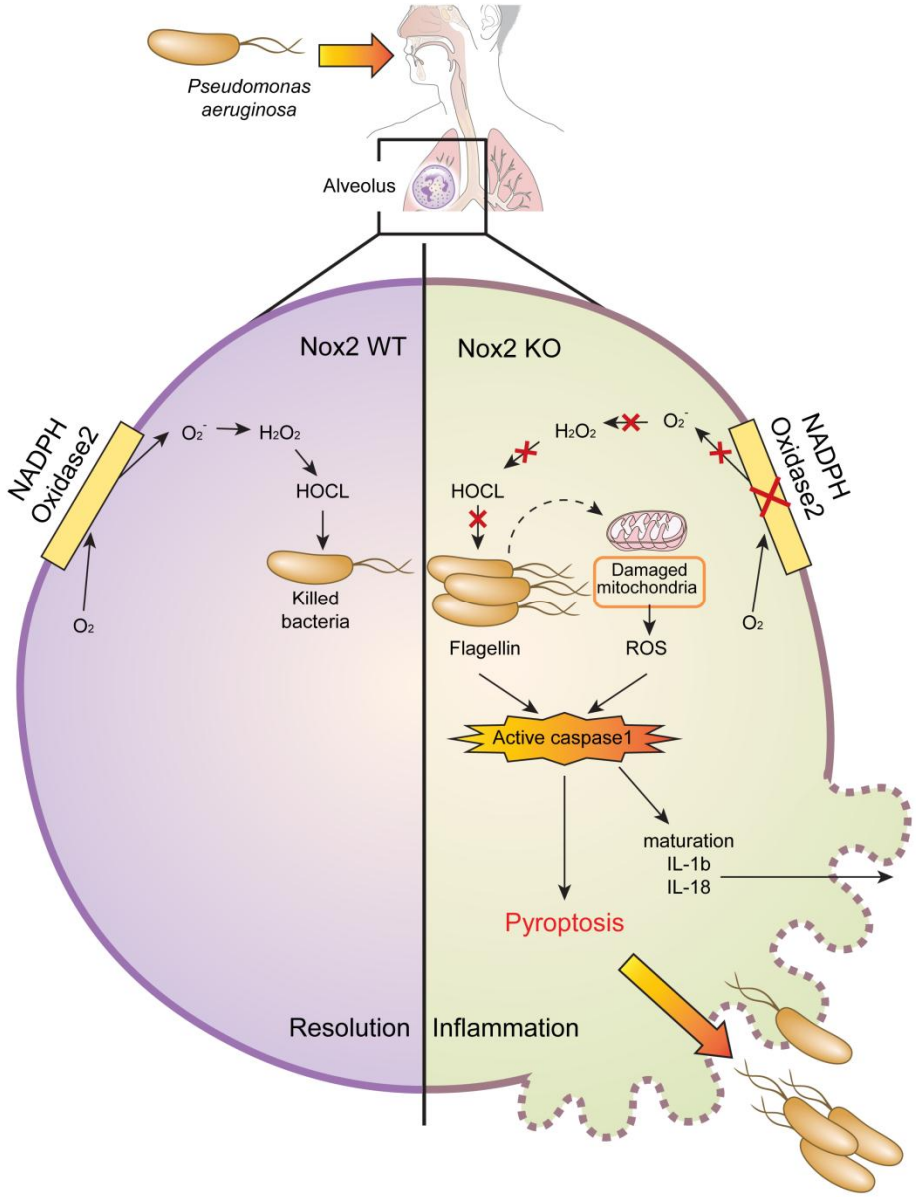

Figure 23. Summary of our study.

IV. DISCUSSION

Recently, NLRC4-dependent inflammasome activation in neutrophils, rather than macrophages, was shown to be responsible for *Salmonella* clearance after challenge,[23] supporting our results that neutrophils play a critical role in host protection. However, in this reports, host protection achieved by neutrophils is mediated by NLRC4/CASP1-dependent IL-1β secretion, but not pyroptosis.[23] Although macrophage pyroptosis is essential for host protection because it releases pathogens from macrophages into the extracellular environment, the role of neutrophil pyroptosis in host protection is controversial. If neutrophil-ingested pathogens can resist typical neutrophil antimicrobial responses, such as the generation of reactive oxygen species and degranulation, the absence of neutrophil pyroptosis may ultimately provide a niche for survival. Indeed, several studies have reported that *Salmonella*,[27] *Staphylococcus aureus*,[28] *Nesisseria gonorrhoeae*,[29] *Chlamydia pneumonia*,[30] and *Anaplasma phagocytophilum*[31] all replicate efficiently within neutrophils, thereby avoiding the immune system. In our study, an almost negligible amount of pyroptotic neutrophils (about 1.5% of the total neutrophils in the bronchoalveolar space) was observed during PAO1 lung infection. Interestingly, neutrophil pyroptosis was dramatically increased in *Nox2*$^{-/-}$ mice upon infection (about 11% of the total neutrophils in the bronchoalveolar

space). The increased pyroptosis in neutrophils devoid of antimicrobial activity suggests that high pathogen burdens induce pyroptosis in neutrophils.

Cytosolic bacterial flagellin in intracellular pathogens such as *S. typhimurim* and *L. pneumophila* is the major trigger of the host immune response; this signaling occurs through the NLRC4 inflammasome.[6,11,12,32] Although NLRC4 is critical for host immune responses against extracellular pathogens such as *P. aeruginosa*,[33,34] *P. aeruginosa* flagellin is not required to activate the NLRC4 inflammasome in macrophages, even though proteins secreted through the type III secretion system are critical for inducing CASP1 activation via NLRC4.[35] In contrast, during acute lung infection, *P. aeruginosa* flagellin is responsible for host pathological damage via CASP1 activation and IL-1β secretion in macrophages.[21] Although the immunological function of *P. aeruginosa* flagellin is well-defined in macrophages, its role in host immunity in neutrophils has not yet been clearly defined. Here we demonstrated a critical role of PAO1 flagellin for inflammasome activation in neutrophils by showing that the increases in secretion of IL-1β and IL18, neutrophil pyroptosis, and lung injury in infected *Nox2*$^{-/-}$ mice were all significantly attenuated by infection with PAO1Δ*fliC*. However, we could not determine the precise role of NLRC4 in inflammasome activation and host physiology in the absence of NOX2 during PAO1 lung infection. Instead, we founded that NLRC4 induces inflammasome activation in neutrophils during

PAO1 infection. In support of this finding, we showed that the increased levels of pyroptosis and IL-1β secretion observed in PAO1-infected WT BMDNs were blunted in PAO1-infected *Nlrc4*$^{-/-}$ BMDNs. However, interestingly, the increased level of pyroptosis observed in PAO1-infected WT BMDNs was also observed in infected *Nlrp3*$^{-/-}$ BMDNs, while the increase in IL-1β secretion was blunted in *Nlrp3*$^{-/-}$ BMDNs. Though several reports indicate that the NLRP3 inflammasome is involved in IL-1β processing in neutrophils,[36-38] the precise reasons why NLRP3 in neutrophil is responsible for IL-1β processing, but not pyroptosis, in our study remain to be further investigated. However, given that murine CASP11 promotes IL-1β processing via the NLRP3-CASP1 signaling pathway in a manner independent of NLRC4-CASP1 signaling,[39] signaling pathway upstream of NLRP3 such as CASP11 may activate NLRP3-mediated IL-1β secretion, independent of NLRC4-CASP1 signaling, in infected neutrophils.

Although it is well known that *P. aeruginosa* flagellin is recognized by TLR5 in addition to NLRC4,[26] TLR5 is not required for CASP1 activation in response to *P. aeruginosa*. Moreover, *Tlr5*$^{-/-}$ macrophages still demonstrated IL-1β secretion and cell death.[33] To date, the precise role of TLR5 in inflammasome activation in *P. aeruginosa*-infected neutrophils has not yet been defined. However, TLR5 was shown to be highly expressed in infiltrated neutrophils in two human lung diseases commonly associated with chronic *P.*

aeruginosa infection, cystic fibrosis (CF) and bronchiectasis.[40] In addition, TLR5 is stored intracellularly in neutrophils and translocated to the cell surface through cooperative TLR1 and TLR2 signaling.[40] This report supports our findings that TLR5 is responsible for PAO1-induced neutrophil pyroptosis, which is based on our experiments using *Tlr5*$^{+/+}$ and *Tlr5*$^{-/-}$ BMDNs. Since the extent of pyroptosis reduction achieved with PAO1Δ*fliC* infection was almost equal to the sum of the extent of pyroptosis reduction in infected *Nlrc4*$^{-/-}$ BMDNs and the extent of reduction in infected *Tlr5*$^{-/-}$ BMDNs, PAO1-induced neutrophil pyroptosis might be triggered by cooperative recognition of PAO1 flagellin by TLR5 and NLRC4. However, although TLR5 is clearly responsible for PAO1 uptake by infected neutrophils, it remains the scope of future studies to determine whether intracellular TLR5 is directly involved in PAO1-induced neutrophil pyroptosis.

Our study demonstrated previously unknown mechanisms of neutrophil pyroptosis during acute lung infection with *P. aeruginosa* and shed light on the pathological role of this process. Thus, inhibitors that specifically target neutrophil pyroptosis are likely to be useful for curing highly intractable *P. aeruginosa* infections most commonly seen in patients with neutrophil function disorders.

V. **CONCLUSION**

Our study reveals previously unknown mechanisms of neutrophil pyroptosis during *P. aeruginosa* lung infection and clarifies the physiological role of this process. Furthermore, our findings regarding neutrophil pyroptosis in the context of neutrophil dysfunction may explain the causes of acute and/or chronic infectious diseases discovered in immune-compromised patients.

REFERENCES

1. Britigan BE, Rasmussen GT, Cox CD. Augmentation of oxidant injury to human pulmonary epithelial cells by the Pseudomonas aeruginosa siderophore pyochelin. Infection and immunity 1997;65:1071-6.
2. Hauser AR. Ventilator-associated pneumonia caused by Pseudomonas aeruginosa: cap your needles! Critical care medicine 2012;40:2503.
3. Kurahashi K, Kajikawa O, Sawa T, Ohara M, Gropper MA, Frank DW, et al. Pathogenesis of septic shock in Pseudomonas aeruginosa pneumonia. The Journal of clinical investigation 1999;104:743-50.
4. Koh AY, Priebe GP, Ray C, Van Rooijen N, Pier GB. Inescapable need for neutrophils as mediators of cellular innate immunity to acute Pseudomonas aeruginosa pneumonia. Infection and immunity 2009;77:5300-10.
5. Lavoie EG, Wangdi T, Kazmierczak BI. Innate immune responses to Pseudomonas aeruginosa infection. Microbes and Infection 2011;13:1133-45.
6. Miao EA, Mao DP, Yudkovsky N, Bonneau R, Lorang CG, Warren SE, et al. Innate immune detection of the type III secretion apparatus

through the NLRC4 inflammasome. Proceedings of the National Academy of Sciences 2010;107:3076-80.

7. Miao EA, Alpuche-Aranda CM, Dors M, Clark AE, Bader MW, Miller SI, et al. Cytoplasmic flagellin activates caspase-1 and secretion of interleukin 1β via Ipaf. Nature immunology 2006;7:569-75.

8. Franchi L, Amer A, Body-Malapel M, Kanneganti T-D, Özören N, Jagirdar R, et al. Cytosolic flagellin requires Ipaf for activation of caspase-1 and interleukin 1β in salmonella-infected macrophages. Nature immunology 2006;7:576-82.

9. Zhao Y, Yang J, Shi J, Gong Y-N, Lu Q, Xu H, et al. The NLRC4 inflammasome receptors for bacterial flagellin and type III secretion apparatus. Nature 2011;477:596-600.

10. Halff EF, Diebolder CA, Versteeg M, Schouten A, Brondijk THC, Huizinga EG. Formation and structure of a NAIP5-NLRC4 inflammasome induced by direct interactions with conserved N-and C-terminal regions of flagellin. Journal of Biological Chemistry 2012;287:38460-72.

11. Broz P, Newton K, Lamkanfi M, Mariathasan S, Dixit VM, Monack DM. Redundant roles for inflammasome receptors NLRP3 and

NLRC4 in host defense against Salmonella. The Journal of experimental medicine 2010;207:1745-55.

12. Pereira MS, Morgantetti GF, Massis LM, Horta CV, Hori JI, Zamboni DS. Activation of NLRC4 by flagellated bacteria triggers caspase-1–dependent and–independent responses to restrict Legionella pneumophila replication in macrophages and in vivo. The Journal of Immunology 2011;187:6447-55.

13. Chen KW, Schroder K. Antimicrobial functions of inflammasomes. Current opinion in microbiology 2013;16:311-8.

14. Franchi L, Muñoz-Planillo R, Núñez G. Sensing and reacting to microbes through the inflammasomes. Nature immunology 2012;13:325-32.

15. Netea MG, Simon A, van de Veerdonk F, Kullberg B-J, Van der Meer JW, Joosten LA. IL-1β processing in host defense: beyond the inflammasomes. PLoS Pathog 2010;6:e1000661.

16. Miao EA, Leaf IA, Treuting PM, Mao DP, Dors M, Sarkar A, et al. Caspase-1-induced pyroptosis is an innate immune effector mechanism against intracellular bacteria. Nature immunology 2010;11:1136-42.

17. Bergsbaken T, Fink SL, Cookson BT. Pyroptosis: host cell death and inflammation. Nature Reviews Microbiology 2009;7:99-109.

18. Labbe K, Saleh M. Cell death in the host response to infection. Cell Death & Differentiation 2008;15:1339-49.

19. Lamkanfi M, Dixit VM. Manipulation of host cell death pathways during microbial infections. Cell host & microbe 2010;8:44-54.

20. Faure E, Mear J-B, Faure K, Normand S, Couturier-Maillard A, Grandjean T, et al. Pseudomonas aeruginosa type-3 secretion system dampens host defense by exploiting the NLRC4-coupled inflammasome. American journal of respiratory and critical care medicine 2014;189:799-811.

21. Cohen TS, Prince AS. Activation of inflammasome signaling mediates pathology of acute P. aeruginosa pneumonia. The Journal of clinical investigation 2013;123:1630-7.

22. Mackay IR, Rosen FS, Lekstrom-Himes JA, Gallin JI. Immunodeficiency diseases caused by defects in phagocytes. New England Journal of Medicine 2000;343:1703-14.

23. Chen KW, Groß CJ, Sotomayor FV, Stacey KJ, Tschopp J, Sweet MJ, et al. The neutrophil NLRC4 inflammasome selectively promotes IL-1β maturation without pyroptosis during acute Salmonella challenge. Cell reports 2014;8:570-82.

24. Lightfield KL, Persson J, Trinidad NJ, Brubaker SW, Kofoed EM, Sauer J-D, et al. Differential requirements for NAIP5 in activation of the NLRC4 inflammasome. Infection and immunity 2011;79:1606-14.

25. Verma A, Arora SK, Kuravi SK, Ramphal R. Roles of specific amino acids in the N terminus of Pseudomonas aeruginosa flagellin and of flagellin glycosylation in the innate immune response. Infection and immunity 2005;73:8237-46.

26. Feuillet V, Medjane S, Mondor I, Demaria O, Pagni PP, Galán JE, et al. Involvement of Toll-like receptor 5 in the recognition of flagellated bacteria. Proceedings of the National Academy of Sciences 2006;103:12487-92.

27. Geddes K, Cruz III F, Heffron F. Analysis of cells targeted by Salmonella type III secretion in vivo. PLoS Pathog 2007;3:e196.

28. Rogers DE, Tompsett R. The survival of staphylococci within human leukocytes. The Journal of experimental medicine 1952;95:209-30.

29. Casey S, Shafer W, Spitznagel J. Neisseria gonorrhoeae survive intraleukocytic oxygen-independent antimicrobial capacities of anaerobic and aerobic granulocytes in the presence of pyocin lethal for extracellular gonococci. Infection and immunity 1986;52:384-9.

30. van Zandbergen G, Gieffers J, Kothe H, Rupp J, Bollinger A, Aga E, et al. Chlamydia pneumoniae multiply in neutrophil granulocytes and

delay their spontaneous apoptosis. The Journal of Immunology 2004;172:1768-76.

31. Chen S-M, Dumler JS, Bakken JS, Walker DH. Identification of a granulocytotropic Ehrlichia species as the etiologic agent of human disease. Journal of Clinical Microbiology 1994;32:589-95.

32. Pereira MS, Marques GG, DelLama JE, Zamboni DS. The Nlrc4 inflammasome contributes to restriction of pulmonary infection by flagellated Legionella spp. that trigger pyroptosis. The inflammasome and its role in infections 2011:83.

33. Franchi L, Stoolman J, Kanneganti TD, Verma A, Ramphal R, Núñez G. Critical role for Ipaf in Pseudomonas aeruginosa-induced caspase-1 activation. European journal of immunology 2007;37:3030-9.

34. Miao EA, Ernst RK, Dors M, Mao DP, Aderem A. Pseudomonas aeruginosa activates caspase 1 through Ipaf. Proceedings of the National Academy of Sciences 2008;105:2562-7.

35. Sutterwala FS, Mijares LA, Li L, Ogura Y, Kazmierczak BI, Flavell RA. Immune recognition of Pseudomonas aeruginosa mediated by the IPAF/NLRC4 inflammasome. The Journal of experimental medicine 2007;204:3235-45.

36. Bakele M, Joos M, Burdi S, Allgaier N, Pöschel S, Fehrenbacher B, et al. Localization and functionality of the inflammasome in neutrophils. Journal of Biological Chemistry 2014;289:5320-9.

37. Mankan AK, Dau T, Jenne D, Hornung V. The NLRP3/ASC/Caspase-1 axis regulates IL-1β processing in neutrophils. European journal of immunology 2012;42:710-5.

38. Cho JS, Guo Y, Ramos RI, Hebroni F, Plaisier SB, Xuan C, et al. Neutrophil-derived IL-1β is sufficient for abscess formation in immunity against Staphylococcus aureus in mice. PLoS Pathog 2012;8:e1003047.

39. Kayagaki N, Warming S, Lamkanfi M, Walle LV, Louie S, Dong J, et al. Non-canonical inflammasome activation targets caspase-11. Nature 2011;479:117-21.

40. Koller B, Kappler M, Latzin P, Gaggar A, Schreiner M, Takyar S, et al. TLR expression on neutrophils at the pulmonary site of infection: TLR1/TLR2-mediated up-regulation of TLR5 expression in cystic fibrosis lung disease. The Journal of Immunology 2008;181:2753-63.

ABSTRACT (in Korean)

녹농균으로 인한 폐 감염시 Nox2 유무에 따른 호중구 pyroptosis 의 작용 기전 연구

<지도교수 유지환>

연세대학교 대학원 의과학과

류재찬

대식세포에서 세포 내 병원균을 효과적으로 처리하기 위한 작용기작으로 NLRC4 inflammasome 의 활성화에 의한 caspase-1 의존적인 pyroptosis 가 중요한 역할을 한다는 사실은 알려져 있다. 하지만 세균의 급성 감염에서 중요한 역할을 하는 호중구에서의 NLRC4 inflammasome 에 의한 pyroptosis 에 대한 연구는 아직까지 잘 되어 있지 않다.

따라서 본 연구를 통해 녹농균으로 인한 폐 감염 시 호중구 특이적인 조절 작용과 병적인 역할에 대해 알아보려고 하였다. Nox2 결손 유전자 마우스 모델을 이용해서 확인한 결과 nox2 가 없을 시 녹농균에 대한 호중구의 항균 작용이 현저하게 감소되어 있었으며 pyroptosis 또한 증가되어 있었다. 그리고 이런 호중구의

pyroptosis 증가는 녹농균의 병원성 물질 중 하나인 flagellin 에 의한 것이었음을 flagellin 이 결손된 균주를 이용해서 확인하였다. 녹농균으로 인한 호중구의 pyroptosis 가 NLRC4 와 TLR5 의존적이라는 사실 또한 각각의 유전자 결손 마우스 모델을 통해 확인할 수 있었다.

본 연구를 통해 녹농균으로 인한 폐 감염 모델에서 호중구 pyroptosis 의 작용기전을 밝혀내었다. 이 결과는 호중구의 기능에 문제가 있는 환자들에게서 급성 감염이 발생할 경우 호중구의 pyroptosis 가 중요한 역할을 할 수 있을 것이라는 가능성을 제시한다.

핵심되는 말: 녹농균, 호중구, pyroptosis, nlrc4, inflammasome, 플라젤린

PUBLICATION LIST

1. Ryu J, Kim M, Kwon Y, Oh J, Yoon S, Shin S, et al. Neutrophil pyroptosis mediates pathology of P. aeruginosa lung infection in the absence of the NADPH oxidase NOX2. Mucosal Immunology 2016.
2. Chen X, Lee K-A, Ren X, Ryu J-C, Kim G, Ryu J-H, et al. Synthesis of a highly HOCl-selective fluorescent probe and its use for imaging HOCl in cells and organisms. Nature Protocols 2016;11:1219-28.
3. Lee K, Lee K-M, Go J, Ryu J-C, Ryu J-H, Yoon SS. The ferrichrome receptor A as a new target for Pseudomonas aeruginosa virulence attenuation. FEMS microbiology letters 2016;363:fnw104.